

# Surfactant-controlled aqueous synthesis of SnO<sub>2</sub> nanoparticles via the hydrothermal and conventional heating methods

Muhammad Akhyar FARRUKH<sup>1,2</sup>, Boon-Teck HENG<sup>1</sup>, Rohana ADNAN<sup>1,\*</sup>

<sup>1</sup>*School of Chemical Sciences, Universiti Sains Malaysia, 11800 Penang, MALAYSIA*

*e-mail address: r\_adnan@usm.my*

<sup>2</sup>*Permanent address: Department of Chemistry, GC University Lahore, PAKISTAN*

*e-mail: akhyar100@gmail.com*

Received 15.01.2010

Tin oxide nanoplates and nanoballs were fabricated using a cationic surfactant of cetyltrimethylammonium bromide (CTABr) as an organic supramolecular template and tin(IV) chloride as an inorganic precursor via the hydrothermal and conventional heating methods. Urea, which decomposes to ammonium and hydroxide ions during hydrolysis, was used as the source of slow homogeneous precipitation of Sn<sup>4+</sup> with OH<sup>-</sup> to control the particle size. The influence of different reaction parameters (time, temperature, and ratio of Sn<sup>4+</sup> to CTABr) on particle sizes, particle distribution, and morphology was investigated using X-ray diffraction (XRD), transmission electron microscopy (TEM), and Fourier transform infrared (FTIR) spectroscopy. XRD data showed that the size of the SnO<sub>2</sub> nanoparticles decreased with increasing reaction time using the conventional heating method, while no significant change was observed with the hydrothermal method. Nanoplates with average sizes of 9.36 nm and nanoballs up to 4.51 nm were prepared using different ratios of Sn<sup>4+</sup> to CTABr at different temperatures and reaction times by the hydrothermal and conventional heating methods, respectively. Elimination of surfactant from tin-surfactant composites by calcination yielded a porous tin oxide nanostructure.

**Key Words:** Nanostructures, chemical synthesis, nanoplates, nanoballs, X-ray diffraction, electron microscopy

## Introduction

Tin oxide (SnO<sub>2</sub>) is an important n-type semiconducting material with a band gap of 3.65 eV. It has been widely used in many applications such as optoelectronic devices,<sup>1</sup> fabricating solar cells,<sup>2,3</sup> electrochemical

---

\*Corresponding author

applications,<sup>4</sup> electrode materials for Li-ion batteries,<sup>5</sup> catalysts for redox reactions,<sup>6,7</sup> and gas sensors.<sup>8–11</sup> Due to its high sensitivity to reduce as well as to oxidize gases, SnO<sub>2</sub> has been used as the predominant sensing material in the field of solid-state gas sensors for environmental monitoring of CO, H<sub>2</sub>, and NO. The large surface area of SnO<sub>2</sub> allows more surface to be available for CO adsorption and the subsequent desorption of CO<sub>2</sub>, which in turn would allow for an increase in its sensitivity.<sup>12,13</sup> Nanosized SnO<sub>2</sub> could enhance the sensor performance because of its microstructural characteristics and electronic properties. Nanometer-sized metal and semiconductor particles have a large potential for industrial applications. Mesoporous materials can be derived using supramolecular assemblies of cationic surfactants such as cetyltrimethylammonium bromide (CTABr), which act as templates of the inorganic components during synthesis.<sup>14</sup> Their large surface areas and narrow pore size distributions make them ideal candidates for catalysts, molecular sieves, and electrodes in solid-state ionic devices.<sup>15</sup>

A number of researchers have reported the use of surfactants in the synthesis of nanosized metal oxides. A cationic surfactant was employed in the synthesis of chromium oxide nanocrystals via solid thermal decomposition to induce generation of mesopores,<sup>12</sup> and the synthesis of CeO<sub>2</sub> nanoplates, nanorods, and nanotubes by the hydrothermal method was reported by Pan et al.<sup>16</sup> The mesoporous particles synthesized by CTABr possessed a uniform pore size caused by the strong interaction between templates and precursors. According to Sarkar et al.,<sup>17</sup> an optimized amount of surfactant can achieve high specific surface area and narrow pore size. Certain surfactants are toxic and lead to impurities in the final product, but surfactant can be removed by washing with ethanol or water and through calcinations at high temperatures to increase the purities of the final product.<sup>12,14,15,18</sup> Acarbas et al.<sup>19</sup> reported that the tin oxide used for gas sensors has been synthesized by various methods, such as direct strike precipitation,<sup>20</sup> 2-step solid state synthesis,<sup>21</sup> microemulsion,<sup>22</sup> sol-gel,<sup>23</sup> spray pyrolysis,<sup>24</sup> gel combustion technique,<sup>25</sup> and hydrothermal synthesis.<sup>26</sup>

Controlled precipitation is best accomplished via homogeneous precipitation, which utilizes chemical reactions such as urea decomposition, whose kinetic rate limits the release of supersaturating species.<sup>27</sup> The homogeneous precipitation method uses urea as a reagent to control the pH and to obtain a pure and dense hydrous tin oxide.<sup>28</sup> When urea is gently heated to about 85 °C, it decomposes slowly during the release of the ammonia and carbonate ions into the solution. This uniform rise in pH results in the nucleation and growth of uniformly sized and shaped particles.<sup>20</sup> The hydrothermal method is an alternative to calcination for the crystallization of SnO<sub>2</sub> at mild temperatures,<sup>12</sup> and it is one of the best methods for producing fine oxide powders.<sup>28</sup> In hydrothermal synthesis, water is used as a catalyst and as a component of solid phases at elevated temperatures and pressures.<sup>29</sup> The use of an expensive autoclave is a disadvantage of hydrothermal synthesis.

CTABr-assisted nanosized SnO<sub>2</sub> has been prepared with a variety of methods by using NH<sub>4</sub>OH at room temperature and the hydrothermal method,<sup>14,30,31</sup> the water-in-oil microemulsion-assisted method,<sup>32</sup> and the 2-step templating method.<sup>33</sup> The rod-like structure<sup>31</sup> and wormhole-like phases of SnO<sub>2</sub><sup>34</sup> have been reported when using a counterion source of NaOH and NH<sub>4</sub>OH, respectively. In this paper, the use of the less expensive conventional heating method as well as the hydrothermal method is discussed. CTABr was used as an organic template, SnCl<sub>4</sub>·5H<sub>2</sub>O as the inorganic precursor, and urea as the source for OH<sup>-</sup>. The effects of reaction time, temperature, and the ratio of cationic surfactant (CTABr) to tin(IV) on the particles sizes, particles distribution, and morphology (platelet and ball-like) were also studied.

## Experimental

### Chemicals

The chemical reagents used were cetyltrimethylammonium bromide (CTABr) ( $C_{16}H_{33}N(CH_3)_3Br$ ) from Sigma, hydrated tin chloride ( $SnCl_4 \cdot 5H_2O$ ) from Riedel-de Haen, ultrapure water from SQ-Ultra Pure Water Purification System, 99.5% ethanol ( $C_2H_5OH$ ) from System, and 99% urea ( $(NH_2)_2CO$ ) from Riedel-de Haen. All chemicals were used as received without any further purification.

### Synthesis procedure

*Hydrothermal method:* In the hydrothermal method, for a 1:1 ratio of  $Sn^{4+}$  to CTABr, 3.505 g (10 mmol) of hydrate tin chloride, 3.639 g (10 mmol) of cationic surfactant (CTABr), and 9.789 g of urea were dissolved in 100 mL of distilled water in a beaker under continuous stirring. The solution was stirred to homogeneity, and then the mixture was transferred to a 100 mL Teflon-lined autoclave. The solution was heated in an oven at 100 °C for 24 h. The resulting product was washed with ethanol and water via centrifugation (7000 rpm) to remove any impurities, and then dried in an oven at 80 °C overnight. The dried solids were ground into powder using a mortar and pestle before calcination at 400 °C for 6 h. The above procedure was repeated for molar ratios of 1:3 and 1:5 between  $Sn^{4+}$  and CTABr, reaction times of 48 and 72 h, and temperatures of 120 and 140 °C; see Table.

**Table.** Summary of reaction parameters and methods used in the preparation of tin oxide nanoparticles, as well as particle sizes.

Method	Molar ratio of $Sn^{4+}$ to CTABr	Reaction time (h)	Temperature (°C)	Particle size (nm) by XRD	Particle size (nm) by TEM
A <sup>a</sup>	1:1, 1:3	24, 48, 72	100, 120, 140	9.98	9.81
A	1:5	24	100	9.98	9.67
A	1:5	24	140	9.98	9.36
A	1:5	48	100, 120, 140	9.98	9.82
A	1:5	72	100	9.98	9.39
A	1:5	72	140	9.98	9.48
B <sup>b</sup>	1:1	24	100	9.98	9.87
B	1:1	48	100	6.98	6.93
B	1:1	72	100	5.37	4.51
B	1:3	48	100	9.97	8.77
B	1:5	24, 48, 72	100	9.97	9.91

<sup>a</sup>hydrothermal method, <sup>b</sup>conventional heating method. Average particle size was calculated with more than 250 particles by TEM.

*Conventional heating method:* The mixture was prepared in the same way as the hydrothermal method, but it was transferred into a 100 mL Erlenmeyer flask instead of the Teflon-lined autoclave. The mouth of the

Erlenmeyer flask was covered with aluminium foil and the same reaction parameters were used as described in the hydrothermal method. The effect of temperature on SnO<sub>2</sub> particles synthesized by the conventional method cannot be studied at 120 °C or above, as the mixture in the Erlenmeyer flask becomes dry.

## Characterization techniques

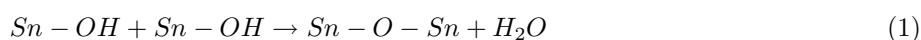
An X-ray diffraction (XRD) diffractometer (X'Pert PRO X-ray diffraction system, Panalytical) was used to investigate the crystalline substance. The sample was ground and pressed into the sample holder and the diffraction pattern was recorded at  $2\theta$ : 20°-80°. Transmission electron microscopy (TEM) images were obtained with Phillip CM12 microscopes at 80 kV. The sample was suspended in ethanol and homogenized with a sonicator for 15 min. One drop of unsettled suspension was put on a copper grid and the solvent was allowed to dry at room temperature. The average particle diameter was calculated from the TEM images by using image analysis software (SIS Soft Imaging GmbH). Fourier transform infrared (FTIR) analyses were performed with a Thermo Nicolet 5700 Spectrometer in the range of 400-4000 cm<sup>-1</sup>.

## Results and discussion

### Characterization by FTIR

The FTIR transmission spectra of SnO<sub>2</sub> synthesized with a 1:1 ratio of Sn<sup>4+</sup> to CTABr at different conditions are shown in Figure 1: a) before calcination, b) after calcination at 400 °C for 6 h, c) pellet put in oven, and d) pellet exposed to air. Figure 1a, the spectrum before calcination, shows that the peaks in the FTIR pattern at about 3300-3430 and 1635-1619 cm<sup>-1</sup> were due to stretching vibrations of water molecules or hydroxide groups absorbed at the surface of the tin oxide.<sup>19,37,38</sup> The bands at 2922, 2841, and 1400 cm<sup>-1</sup> were assigned to C-H stretching and bending vibrations.<sup>12,37</sup> These C-H peaks were attributed to the organic trace residues from the CTABr surfactant. The peak at around 1400 cm<sup>-1</sup> was assigned to NH deformation of ammonia and the NH stretching vibration from decomposition of urea or ammonium hydroxide.<sup>20,38</sup> The bands at around 667 and 554 cm<sup>-1</sup> were attributed to Sn-O stretching modes of Sn-O-Sn and Sn-OH, respectively.<sup>20</sup> These bands show that before calcination, not all Sn(OH)<sub>4</sub> had undergone a condensation reaction to form SnO<sub>2</sub>.

The peaks that appeared before calcination (Figure 1a) and were related to urea, ammonia, or surfactant almost disappeared when the product was calcined at 400 °C for 6 h (Figure 1b). The absence or reduction of intensity of bands at 2922, 2841, and 1400 cm<sup>-1</sup> confirms the removal of surfactant after calcinations at 400 °C for 6 h. After calcinations, the intensity of the bands at 3300-3430 and 1635-1619 cm<sup>-1</sup> was also greatly reduced. This shows the removal of absorbed water molecules and hydroxyl groups during calcinations. The peaks at about 660 and 554 cm<sup>-1</sup> became stronger and weaker, respectively, because a condensation reaction occurred between Sn-OH groups during calcinations to form Sn-O-Sn, as shown in Eq. (1).<sup>19,20,38</sup>



By heating the pellet in the oven and leaving it for 1 day after calcination, the intensity of the bands at 3300-3430 and 1635-1619 cm<sup>-1</sup>, which corresponded to the water molecules absorbed on the surface of SnO<sub>2</sub> from moisture during handling, was reduced (Figure 1c). However, a broad band appeared at around 620 cm<sup>-1</sup>,

which was a characteristic of the oxide-bridge functional group.<sup>37</sup> It was supposed, and confirmed with XRD, that the temperature changed the crystallographic rearrangement of Sn-O-Sn into O-Sn-O during calcinations. When the pellet was exposed to air after calcination, the intensity of the bands at 3300-3430 and 1635-1619  $\text{cm}^{-1}$  was broadened, which correspond to the absorption of water molecules on the surface of the sample from moisture (Figure 1d). The FTIR spectra of tin oxide synthesized by different reaction parameters and methods also exhibited a similar pattern to that shown in Figure 1.

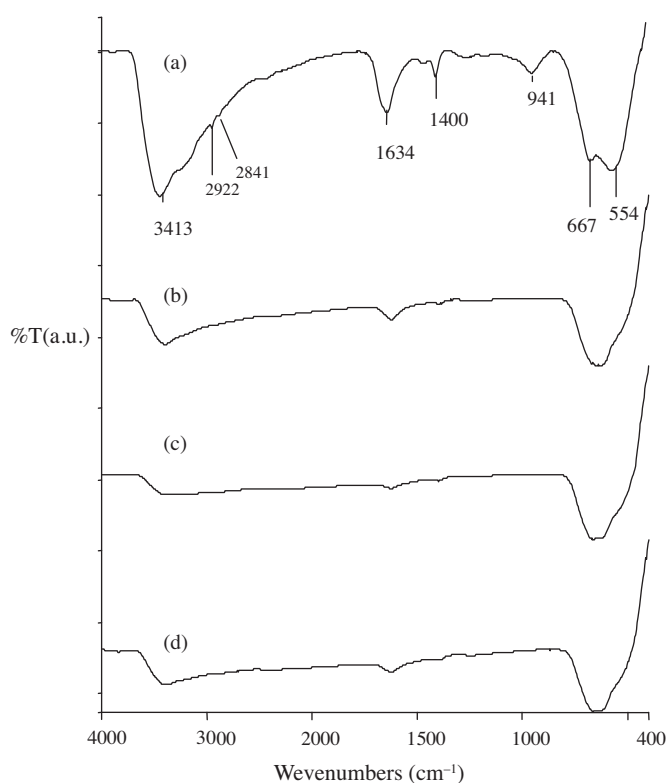


**Figure 1.** FTIR spectra of tin oxide synthesized via the conventional heating method with a  $\text{Sn}^{4+}$  to CTABr ratio of 1:1, heated at 100 °C for 24 h (a) before calcinations, (b) after calcinations, (c) pellet put in oven, and (d) pellet exposed to air.

### The effect of surfactant ratio, reaction time, and temperature

The XRD pattern of  $\text{SnO}_2$  nanoparticles recorded in the region of  $2\theta$  of 20°-80° are displayed in Figure 2. The XRD results showed that all samples had diffraction peaks at 26.6°, 33.9°, and 51.9°, indicating the formation of tin oxide particles. These 3 peaks corresponded to the (110), (101), and (211) reflection planes of a tetragonal lattice of tin oxide as identified using the standard data JCPDS file No. 01-070-6153. No obvious reflection peaks from impurities such as unreacted Sn or SnO were detected, thus indicating the high purity of the product.<sup>39</sup> The crystallite grain size of  $\text{SnO}_2$  could be calculated according to the Scherrer formula using

the half-width of intense (211) reflection peaks:

$$L = \frac{K\lambda}{(\beta \cos \theta)}, \quad (2)$$

where  $L$  is the mean crystalline size,  $\lambda$  is the wavelength of the X-ray radiation ( $\text{Cu K}\alpha = 0.15406 \text{ nm}$ ),  $K$  is a constant taken as 0.89,  $\beta$  is the line width at half the maximum height, and  $\theta$  is the diffracting angle.

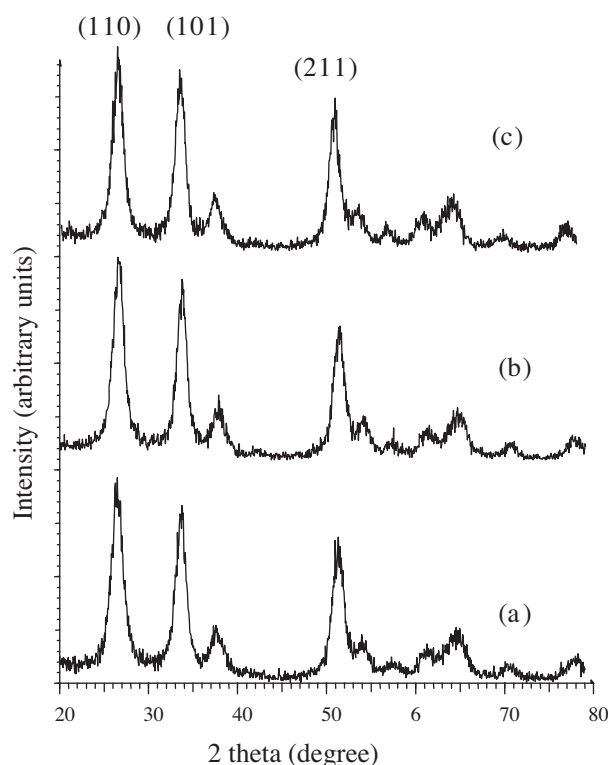


**Figure 2.** XRD diffractogram of tin oxide synthesized via the hydrothermal method with a  $\text{Sn}^{4+}$  to CTABr ratio of 1:5, heated for 48 h at (a) 100 °C, (b) 120 °C, and (c) 140 °C.

*Hydrothermal method:* The XRD patterns of calcined tin oxide synthesized with a 1:5 ratio of  $\text{Sn}^{4+}$  to CTABr and heated for 48 h at temperatures of 100, 120, and 140 °C by the slow decomposition of urea are shown in Figure 2. The XRD diffraction peaks of these 3 different reaction temperatures are sharp and narrow. There were no large differences in the XRD pattern of the  $\text{SnO}_2$  samples produced using the 3 temperatures. Our results show that the increasing of reaction temperature does not have an effect on the crystallite size of tin oxide. The crystallite size of  $\text{SnO}_2$  prepared at 3 different temperatures was 9.98 nm, as calculated by the Scherrer equation (Table). The XRD patterns of  $\text{SnO}_2$  nanoparticles synthesized by using tin to surfactant ratios of 1:1 and 1:3 with reaction times of 24, 48, and 72 h also exhibit similar behavior. This shows that different reaction parameters do not have an effect on the  $\text{SnO}_2$  particle sizes.

Figure 3 shows the typical transmission electron microscopy (TEM) images of the sample prepared at a 1:5 molar ratio of  $\text{Sn}^{4+}$  to CTABr with the reaction time of 24 h and the reaction temperature of 100 °C.

Under these conditions, SnO<sub>2</sub> particles showed a platelet-like morphology, but various sizes of particles were observed (Figure 3a). This shows that a platelet-like morphology of tin oxide can be synthesized when the ratio of Sn<sup>4+</sup> to CTABr ratio is increased to 1:5. The TEM images show that the average diameter of the irregular nanoplates ranges from the smallest nanoplate at 1.73 nm to the largest at 18.62 nm, and many spherical particles coexist with the nanoplatelets. However, the formation of SnO<sub>2</sub> nanorods with a diameter of 40-260 nm has been reported when using NaOH as a source of counterions instead of urea, as in the present work, under hydrothermal conditions.<sup>31</sup> The possible formation of a SnO<sub>2</sub> nanoplate is described as a CTA<sup>+</sup> cation that is firstly absorbed on the surface of SnO<sub>2</sub> nanoparticles; then the exposed surface planes that are not attached by CTA<sup>+</sup> tend to combine to reduce the surface energy to form a cubic plane structure.<sup>16</sup>

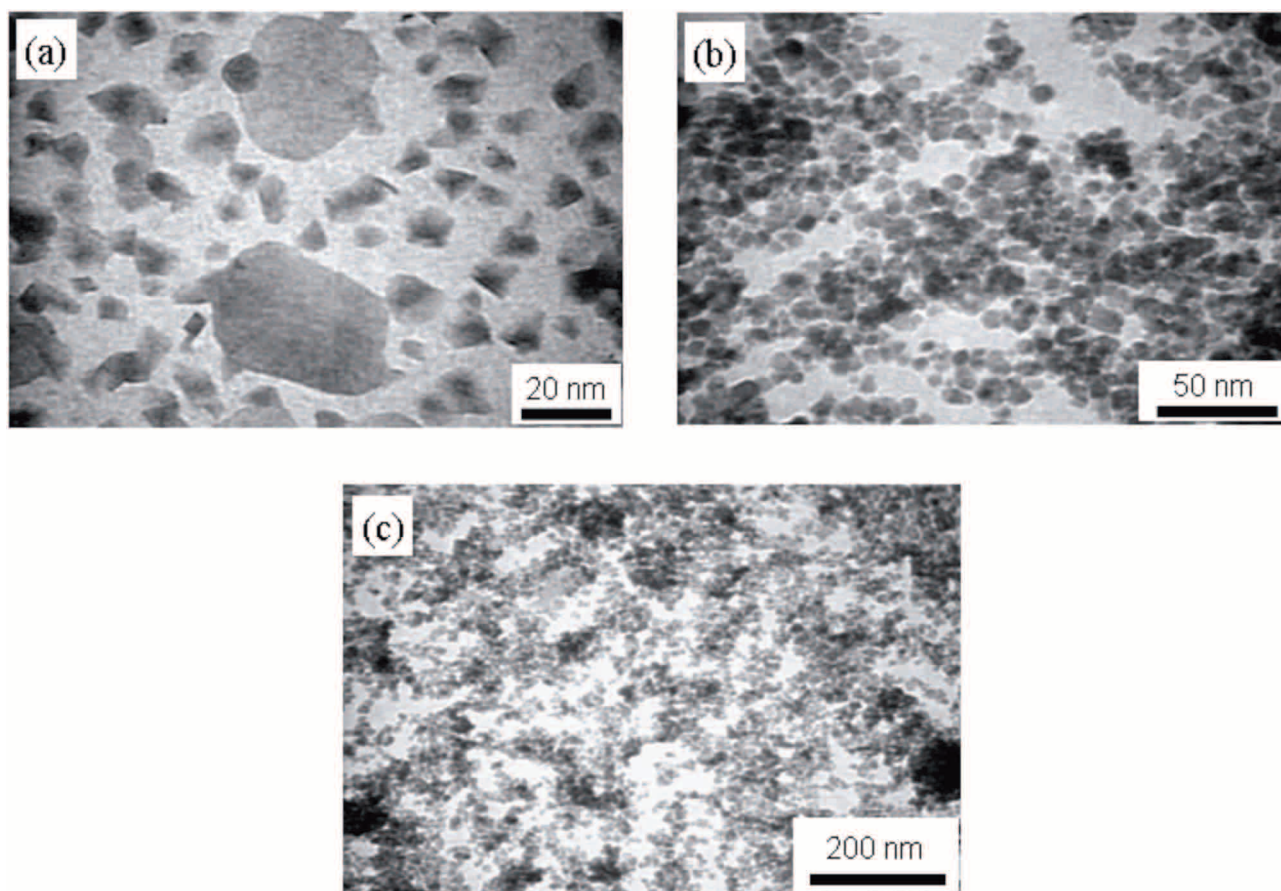


**Figure 3.** TEM images of tin oxide synthesized via the hydrothermal method with a Sn<sup>4+</sup> to CTABr ratio of 1:5, heated at 100 °C for 24 h. (a) nanoplates, (b) mesostructure at scale bar = 50 nm, (c) mesostructure at scale bar = 200 nm.

*Conventional heating method:* Figure 4 shows the XRD pattern of calcined tin oxide synthesized using a Sn<sup>4+</sup> to CTABr ratio of 1:5 by decomposition of urea for 24, 48, and 72 h at 100 °C. The crystallite size of synthesized SnO<sub>2</sub> was around 9.97 nm, as calculated by the Scherrer equation (Table). The crystallite size

obtained in this study was smaller than the 11.1 nm reported when SnO<sub>2</sub> was synthesized in NH<sub>4</sub>OH at a low temperature and without hydrothermal conditions.<sup>30</sup> This shows that different reaction times do not have an effect on the SnO<sub>2</sub> particles sizes with this ratio; it was found to be similar as synthesized via the hydrothermal method. In order to investigate the effect of surfactant ratios and heating time on the crystallization process of SnO<sub>2</sub>, the XRD results of SnO<sub>2</sub> with a 1:1 ratio of Sn<sup>4+</sup> to CTABr for heating times of 24, 48, and 72 h at 100 °C are shown in Figure 5. When the reaction time was increased from 24 to 72 h, the diffraction peaks became broader, which is consistent with the smaller particle sizes. The crystallite size of SnO<sub>2</sub> calculated by the Scherrer equation using the half-width of the (211) reflection peak for 24, 48, and 72 h decreased from 9.98 to 6.98 nm and to 5.37 nm, respectively (Table).

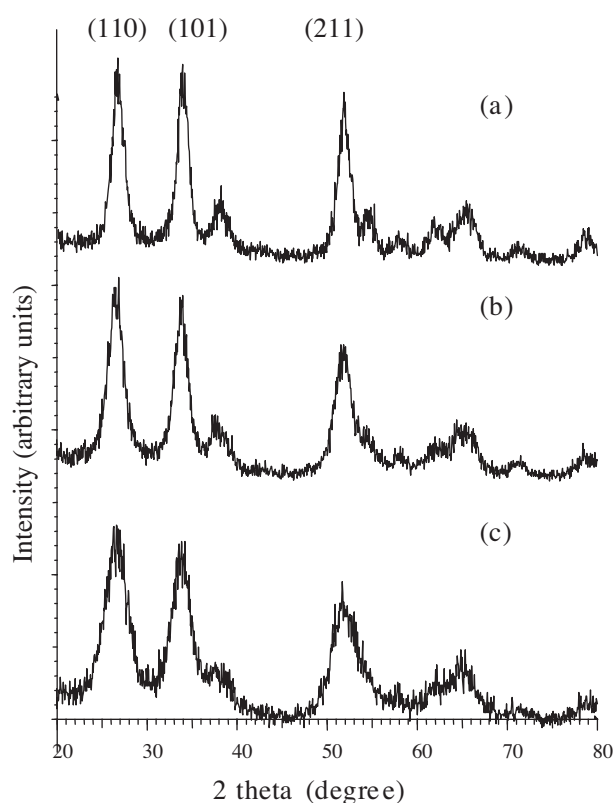


**Figure 4.** XRD diffractograms of tin oxide synthesized via the conventional heating method with a Sn<sup>4+</sup> to CTABr ratio of 1:5, heated at 100 °C for (a) 24 h, (b), 48 h, and (c) 72 h.

TEM images of the tin oxide (Figure 6a) clearly show that the homogeneous precipitation method using urea results in the formation of ball-like morphology with average particle size of 4.51 nm as compared to 18.2 nm.<sup>30</sup> The size of the particle diameter of microstructure SnO<sub>2</sub> was reported in the range of 40-60 nm when prepared by the same method, using urea, but without CTABr.<sup>20</sup>



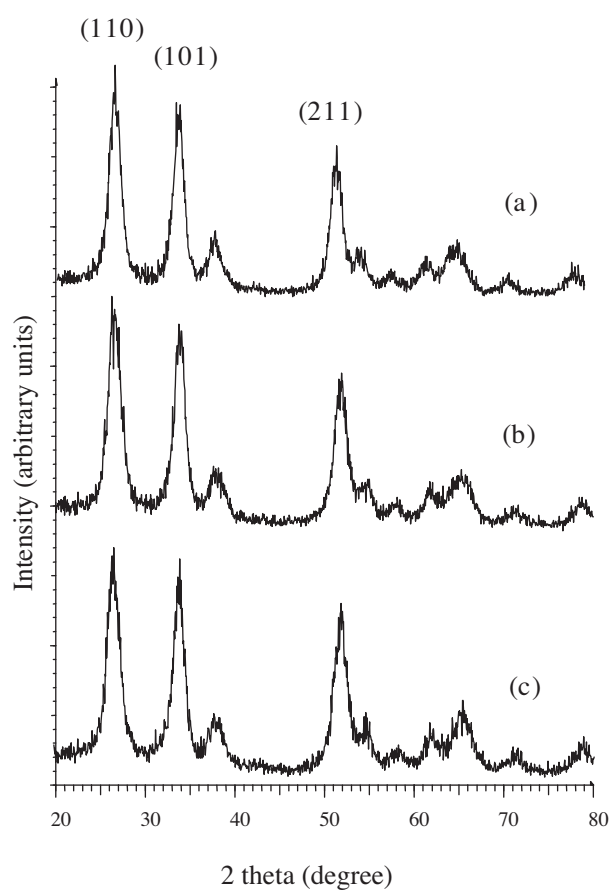


**Figure 5.** XRD diffractogram of tin oxide fabricated via the conventional heating method with a  $\text{Sn}^{4+}$  to CTABr ratio of 1:1, heated at 100 °C for (a) 24 h, (b), 48 h, and (c) 72 h.

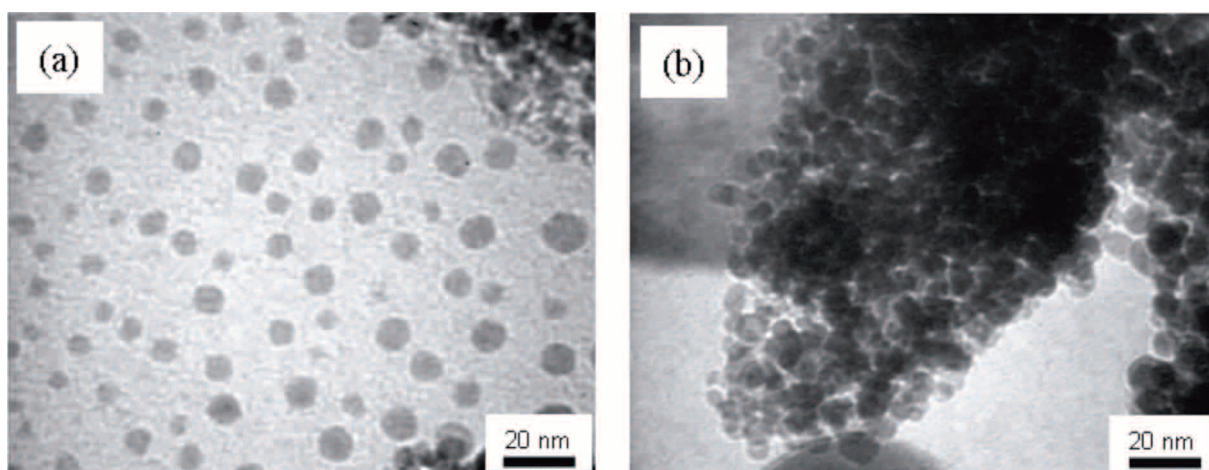


**Figure 6.** TEM images of tin oxide synthesized via the conventional heating method. (a) nanoballs with a  $\text{Sn}^{4+}$  to CTABr ratio of 1:5, heated at 100 °C for 48 h; (b) mesostructure with a  $\text{Sn}^{4+}$  to CTABr ratio of 1:3, heated at 100 °C for 48 h.

The addition of surfactant led to a narrow size distribution of particles, making the nucleation complete at the early stage of the sol-gel process and inhibiting the crystal growth. In the absence of surfactant, the nucleation process is comparatively slow, which results in a broad size distribution of the SnO<sub>2</sub> nanocrystallites.<sup>35</sup> When the concentration of the surfactant is larger than the critical micelle concentration (CMC), the surfactant will form micelles. Agglomerations of particles occur in the micelle formation of surfactant, which results in a larger particle size when the ratio of surfactant increases. The CMC of CTABr is  $9.2 \times 10^{-4}$  M.<sup>36</sup>

A change in crystallite size (nanoplates) was not observed in the hydrothermal method because the nucleation was supposed to be completed at the same rate without affecting the particle size under high pressure, which is enough for the crystal growth at early stage. However, particle size varies in the conventional heating method, and the size of the nanoballs decreases with an increase in reaction time due to the breaking of particles at a high reaction time. Different morphologies of nanoparticles were obtained with both methods, which demonstrates that the shape of SnO<sub>2</sub> nanoparticles could be controlled by different reaction conditions. At higher pressure (hydrothermal method), SnO<sub>2</sub> shows platelet-like morphology, which might be because of the crystal growth of SnO<sub>2</sub> toward the reflection planes of a tetragonal lattice, which limits the size to ball-like morphology under low pressure (conventional heating method). More work is to be carried out for a concrete understanding of this process.

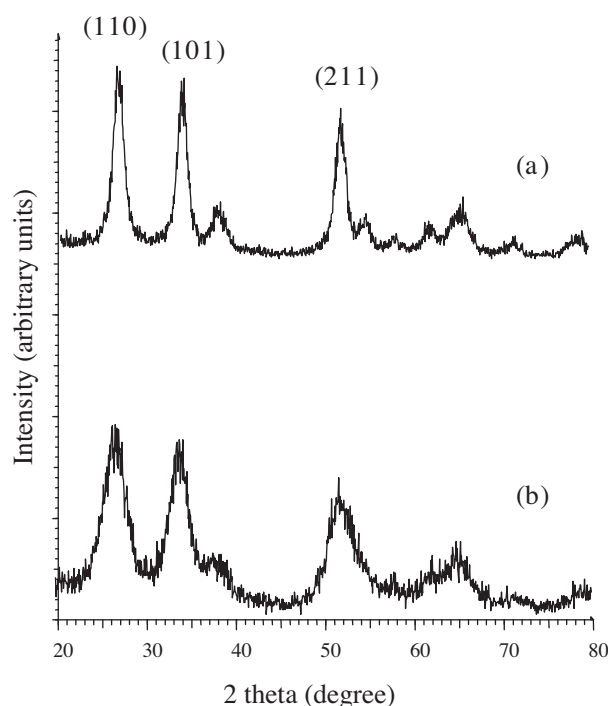
### The effect of preparation methods on particle sizes

Figure 7 shows that the XRD diffraction peaks of SnO<sub>2</sub> synthesized via the conventional heating method are broader than those prepared via the hydrothermal method due to the decrease in crystallite sizes. Tin oxide synthesized via the hydrothermal method with a 1:1 ratio of Sn<sup>4+</sup> to CTABr, heated for 72 h at 100 °C, contains a crystallite size of 9.98 nm. Meanwhile, tin oxide synthesized under the same conditions, using the conventional heating method, contains a crystallite size of 5.37 nm, which is smaller than the tin oxide synthesized by the hydrothermal method. In the hydrothermal method, tin oxide is synthesized under high pressure using a Teflon-coated autoclave, as compared to the conventional heating method, which uses an Erlenmeyer flask. This study shows that smaller particles can be synthesized under lower pressure and in cheaper ways, under controlled conditions.

### Mesostructure of tin oxide

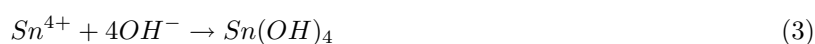
The mesoporous structures of tin oxide synthesized via the hydrothermal and the conventional heating methods are shown by TEM images in Figures 3b and 3c and Figure 6b, respectively. It is indicated that mesopores of tin oxide material are formed by the aggregation of tin oxide nanocrystallites. CTABr surfactant is the main source for forming the mesoporous structure. The FTIR spectra of SnO<sub>2</sub> (Figure 1b) shows the absence or reduction of intensity of bands at 2922, 2841, and 1400 cm<sup>-1</sup> for typical C-H stretching and bending vibrations, which confirms the removal of surfactant after calcinations at 400 °C for 6 h. CTABr surfactant was used as a template that was burnt off at the higher temperature to produce a mesoporous material.<sup>40</sup> The mesopores are formed by eliminating or burning off CTABr from the Sn-CTABr composite.

The mesostructured tin oxide synthesized under acidic conditions is thought to follow the S<sup>+</sup>X<sup>-</sup>I<sup>+</sup> pathway. Where S<sup>+</sup> is the structure director or the CTABr surfactant in this case, I<sup>+</sup> is the inorganic



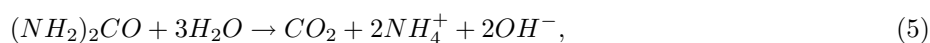
**Figure 7.** XRD diffractograms of calcined tin oxide synthesized with a  $\text{Sn}^{4+}$  to CTABr ratio of 1:1, heated at 100 °C for 72 h via the (a) hydrothermal method and (b) conventional heating method.

precursor and  $\text{X}^-$  is the counterion. Wang et al.<sup>14</sup> proposed a generalized mechanism of formation based on the electrostatic interaction between an inorganic precursor  $\text{I}^+$  and a surfactant head group  $\text{S}^+$ . In this study,  $\text{I}^+$  is the stannum ion,  $\text{Sn}^{4+}$ ;  $\text{S}^+$  is the surfactant templating agent,  $\text{CTA}^+$ ; and  $\text{X}^-$  is the halide ion ( $\text{Cl}^-$ ) and the  $\text{OH}^-$  that serves to buffer the repulsion between the  $\text{S}^+$  and  $\text{I}^+$  by means of a weak hydrogen bonding force. In this work,  $\text{OH}^-$  is supposed to self-assemble around the cationic surfactant head group molecule ( $\text{CTA}^+$ ) so that the  $\text{Sn}^{4+}$  ion can be attracted by the assembled  $\text{OH}^-$  ions to form the mesostructure.<sup>14</sup> In the final step, the template was removed through calcinations at 400 °C for 6 h to generate porosity, as can be observed in the Scheme.<sup>41</sup> This pathway is followed when the concentration of  $\text{OH}^-$  is low or the concentration of CTABr is high (ratios 1:3 and 1:5). Vice versa, free  $\text{OH}^-$  ions remain away from the CTABr molecules and can easily be attracted with  $\text{Sn}^{4+}$  to form insoluble  $\text{Sn}(\text{OH})_4$ . The concentration of urea, which decomposes to  $\text{OH}^-$ , was kept constant in this study; therefore, the concentration of CTABr plays an important template-directed role. However, at a low CTABr concentration (1:1) or a high concentration of  $\text{OH}^-$ , a proposed mechanism for  $\text{SnO}_2$  mesostructure in terms of chemical reaction and crystal growth was described by Chen and Gao<sup>32</sup> and Wen et al.<sup>42</sup> Mesoporous  $\text{SnO}_2$  can be fabricated in an aqueous solution by a hydrolysis-condensation process. Eq. (3) and (4) below describe the possible reaction mechanisms of hydrolysis and condensation, respectively.



where  $\text{OH}^-$  ions are generated from the decomposition of urea and water molecules. It is known that, upon

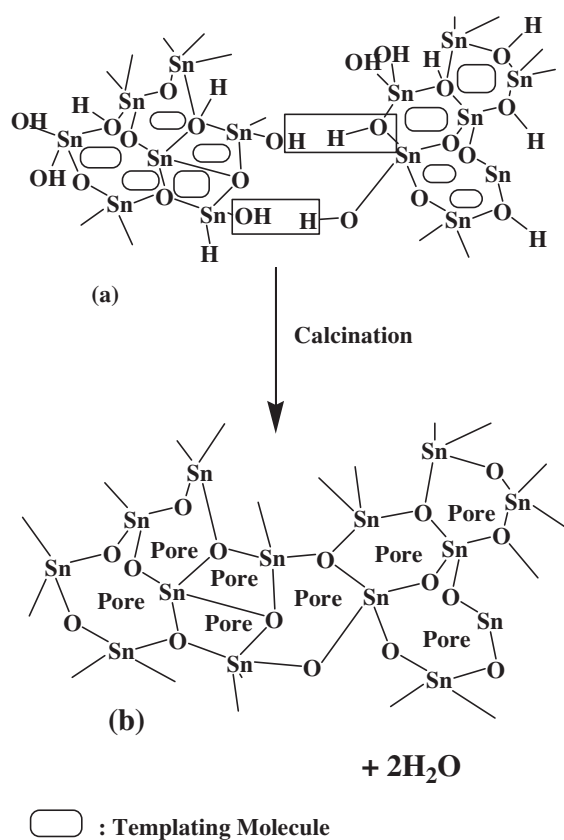
being heated from 80 °C to 100 °C, urea will decompose and produce ammonia and carbon dioxide, as described by Eq. (5):<sup>20</sup>



while the self-decomposition of water can be described by Eq. (6):



where  $K_w$  is the ionic product constant of water, which is  $10^{-14}$ . After a prolonged process, the colloidal particles will link together to form a resulting network of porous structure, as shown in the Scheme.<sup>43</sup>



**Scheme.** Structure of mesoporous tin oxide (a) before calcination and (b) after calcination.

## Conclusions

Various sizes and morphologies of tin oxide (nanoplates, nanoballs, and mesoporous) were successfully prepared via the hydrothermal method and the conventional heating method. Smaller and uniform particles were synthesized via the conventional heating method using urea as a source of  $OH^-$  ions to provide a longer reaction time.  $SnO_2$  nanoparticles were synthesized at sizes of up to 5.37 nm under conditions of a 1:1 ratio of  $Sn^{4+}$  to CTABr for 72 h at 100 °C via the conventional method, as compared to 9.98 nm via the

hydrothermal method (Scherrer formula). SnO<sub>2</sub> nanoplates were synthesized via the hydrothermal method with a Sn<sup>4+</sup> to CTABr ratio of 1:5, heated for 24 h at 100 °C, while nanoballs were prepared via the conventional heating method with a Sn<sup>4+</sup> to CTABr ratio of 1:5, heated for 48 h at 100 °C. It was observed that the morphology of nanoparticles synthesized via the conventional heating method was influenced by changes in the reaction parameters (surfactant ratio, temperature, and time), while no significant change was observed with the hydrothermal method. The cationic surfactant CTABr was used as the template to form mesoporous tin oxide.

## Acknowledgements

The authors would like to acknowledge the School of Chemical Sciences, Universiti Sains Malaysia, and the Malaysian government for support and financial assistance through an eScience research grant (305/PKIMIA/613309). Dr. Muhammad Akhyar Farrukh is a recipient of the TWAS-USM Postdoctoral Fellowship in Research.

## References

1. Kim, T. W.; Lee, D. U.; Choo, D. C.; Kim, J. H.; Kim, H. J.; Jeong, J. H.; Jung, M.; Bahang, J. H.; Park, H. L.; Yoon, Y. S.; Kim, J. Y. *J. Phys. Chem. Solids* **2002**, *63*, 881-885.
2. Moustafid, T. E.; Cachet, H.; Tribollet, B.; Festy, D. *Electrochim. Acta*. **2002**, *47*, 1209-1215.
3. Okuya, M.; Kaneko, S.; Hiroshima, K.; Yaggi, I.; Murakami, K. *J. Eur. Ceram. Soc.* **2001**, *21*, 2099-2102.
4. Chen, F. L.; Liu, M. L. *Chem. Commun.* **1999**, 1829-1830.
5. Kim, C.; Noh, M.; Choi, M.; Cho, J.; Park, B. *Chem. Mater.* **2005**, *17*, 3297-3301.
6. Chou, L.; Cai, Y.; Zhang, B.; Niu, J.; Ji, S.; Li, S. *Appl. Catal. A Gen.* **2003**, *238*, 185-191.
7. Wierchowski, P. T.; Zatorski, L. W. *Appl. Catal. B Environ.* **2003**, *44*, 53-65.
8. Moulson, A. J.; Herbert, J. M. *Electroceramics*, Chapman & Hall, New York, 1990.
9. Shimizu, Y.; Egashira, M. *MRS Bull.* **1999**, *24*, 18-22.
10. Wang, H. C.; Li, Y.; Yang, M. J. *Sens. Actuators. B Chem.* **2006**, *119*, 380-383.
11. Li, G. J.; Zhang, X. H.; Kawi, S. *Sens. Actuators. B Chem.* **1999**, *60*, 64-70.
12. Li, L.; Zhu, Z.; Yao, X.; Lu, G.; Yan, Z. *Micro. Mes. Mater.* **2008**, *112*, 621-626.
13. Sharp, S. L.; Kumar, G.; Vicenzi, E. P.; Bocarsly, A. B. *Chem. Mater.* **1998**, *10*, 880-885.
14. Wang, Y. D.; Ma, C. L.; Su, X. D.; Li, H. D. *Mater. Lett.* **2001**, *51*, 285-288.
15. Zhou, S.; Lu, S.; Ke, Y.; Li, J. *Mater. Lett.* **2003**, *57*, 2679-2681.
16. Pan, C.; Zhang, D.; Shi, L. *J. Solid State Chem.* **2008**, *181*, 1298-1306.
17. Sarkar, A.; Pramanik, S.; Achariya, A.; Pramanik, P. *Micro. Meso. Mater.* **2008**, *115*, 426-431.
18. Firooz, A. A.; Mahjoub, A. R.; Khodadadi, A. A. *Mater. Lett.* **2008**, *62*, 1789-1792.
19. Acarbas, O.; Suvaci, E.; Dogan, A. *Ceram. Int.* **2007**, *33*, 537-542.
20. Song, K. C.; Kang, Y. *Mater. Lett.* **2000**, *42*, 283-289.

21. Li, F.; Chen, L.; Chen, Z.; Xu, J.; Zhu, J.; Xin, X. *Mater. Chem. Phys.* **2002**, *73*, 335-338.
22. Song, K. C.; Kim, J. H. *J. Colloid Interf. Sci.* **1999**, *212*, 193-196.
23. Adnan, R.; Razana, N. A.; Rahman, I. A.; Farrukh, M. A. *J. Chin. Chem. Soc.* **2010**, *57*, 222-229.
24. Lee, J. H.; Park, S. J. *J. Am. Ceram. Soc.* **1993**, *76*, 777-780.
25. Bhagwat, M.; Shah, P.; Ramaswamy, V. *Mater. Lett.* **2003**, *57*, 1604-1611.
26. Baik, N. S.; Sakai, N.; Miura, N.; Yamazoe, N. *J. Am. Ceram. Soc.* **2000**, *83*, 2983-2897.
27. Willard, H. H.; Tang, N. K. *J. Am. Chem. Soc.* **1937**, *59*, 1190-1196.
28. Gordon, L. The precipitation of hydrous oxides of tin and thorium from homogeneous solution by the hydrolysis of non-ionizable compounds, Ph.D. dissertation, The University of Michigan, 1947.
29. Somiya, S.; Roy, R. *Bull. Mater. Sci.* **2000**, *23*, 453-460.
30. Wang, Y. D.; Ma, C. L.; Sun, X. D.; Li, H. D. *Inorg. Chem. Commun.* **2002**, *5*, 751-755.
31. Guo, C.; Cao, M.; Hu, C. *Inorg. Chem. Commun.* **2004**, *7*, 929-931.
32. Chen, D.; Gao, L. *J. Colloid Interf. Sci.* **2004**, *279*, 137-142.
33. Wu, N. L.; Tung, C. Y. *J. Am. Ceram. Soc.* **2004**, *87*, 1741-1746.
34. Wang, Y. D.; Ma, C. L.; Sun, X. D.; Li, H. D. *Inorg. Chem. Commun.* **2001**, *4*, 223-226.
35. Shih, W. J.; Wang, M. C.; Hon, M. H. *J. Cryst. Growth.* **2005**, *275*, e2339-e2344.
36. Zhang, J.; Gao, L. *J. Solid State Chem.* **2004**, *177*, 1425-1430.
37. Xi, L.; Qian, D.; Tang, X.; Chen, C. *Mater. Chem. Phys.* **2008**, *108*, 232-236.
38. Krishnakumar, T.; Pinna, N.; Kumari, K. P.; Perumal, K.; Jayaprakash, R. *Mater. Lett.* **2008**, *62*, 3437-3440.
39. Kim, H.; Shim, S. H. *J. Alloys Compd.* **2006**, *426*, 286-289.
40. Lee A. C.; Lin, R. H.; Yang, C. Y.; Lin, M. H.; Wang, W. Y. *Mater. Chem. Phys.* **2008**, *109*, 275-280.
41. Roger, C.; Hampden-Smith, M. J.; Schaefer, D. W.; Beaucage, G. B. *J. Sol-Gel Sci. Techn.* **1994**, *2*, 67-72
42. Wen, Z.; Wang, Q.; Li, J. *Adv. Funct. Mater.* **2007**, *17*, 2772-2778.
43. Klabunde, K. J. *Nanoscale Materials in Chemistry*, Wiley-Interscience, New York, 2001.